



# Multi-Scale Approach for the Evaluation of Bone Mineralization in Strontium Ranelate-Treated Diabetic Rats

Pedro Álvarez-Lloret<sup>1</sup> · Juan Manuel Fernández<sup>2</sup> · María Silvina Molinuevo<sup>2</sup> · Agustina Berenice Lino<sup>2</sup> · José Luis Ferretti<sup>3</sup> · Ricardo Francisco Capozza<sup>3</sup> · Ana María Cortizo<sup>2</sup> · Antonio Desmond McCarthy<sup>2</sup>

Received: 23 November 2017 / Accepted: 21 March 2018 / Published online: 5 April 2018  
© Springer Science+Business Media, LLC, part of Springer Nature 2018

## Abstract

Long-term diabetes mellitus can induce osteopenia and osteoporosis, an increase in the incidence of low-stress fractures, and/or delayed fracture healing. Strontium ranelate (SrR) is a dual-action anti-osteoporotic agent whose use in individuals with diabetic osteopathy has not been adequately evaluated. In this study, we studied the effects of an oral treatment with SrR and/or experimental diabetes on bone composition and biomechanics. Young male Wistar rats (half non-diabetic, half with streptozotocin/nicotinamide-induced diabetes) were either untreated or orally administered 625 mg/kg/day of SrR for 6 weeks. After sacrifice, femora from all animals were evaluated by a multi-scale approach (X-ray diffraction, Fourier transform infrared spectroscopy, inductively coupled plasma optical-emission spectrometry, static histomorphometry, pQCT, and mechanical testing) to determine chemical, crystalline, and biomechanical properties. Untreated diabetic animals (versus untreated non-diabetic) showed a decrease in femoral mineral carbonate content, in cortical thickness and BMC, in trabecular osteocyte density, in maximum load supported at rupture and at yield point, and in overall toughness at mid-shaft. Treatment of diabetic animals with SrR further affected several parameters of bone (some already impaired by diabetes): crystallinity index (indicating less mature apatite crystals); trabecular area, BMC, and vBMD; maximum load at yield point; and structural elastic rigidity. However, SrR was also able to prevent the diabetes-induced decreases in trabecular osteocyte density (completely) and in bone ultimate strength at rupture (partially). Our results indicate that SrR treatment can partially but significantly prevent some bone structural mechanical properties as previously affected by diabetes, but not others (which may even be worsened).

**Keywords** Diabetes mellitus · Strontium ranelate · Bone mineralization · Microstructural properties · Bone biomechanics

## Introduction

Over the past 25 years, diabetes has also been associated with bone metabolic disorders such as osteopenia and osteoporosis, an increase in the incidence of low-stress

fractures, and delayed fracture healing, a condition that has been termed diabetic osteopathy [1].

Strontium ranelate (SrR) is an orally administered antiosteoporotic agent which has been extensively used for treatment of postmenopausal osteoporosis. SrR is a salt of ranelic acid, including two  $\text{Sr}^{2+}$  ions that can partially substitute  $\text{Ca}^{2+}$  in the hydroxyapatite crystal lattice, and thus be incorporated into bone mineral. SrR has been reported to induce both anabolic and antiresorptive effects on bone metabolism [2]. These combined actions correlate with its beneficial effects on bone mass, bone quality, and bone resistance [3], reducing the risk of vertebral and femoral bone fractures [4, 5]. However, the anti-osteoporotic effects of SrR have not been adequately evaluated in individuals with diabetic osteopathy. After a warning by the European Pharmacovigilance Risk Assessment Committee, important restrictions for the

---

✉ Antonio Desmond McCarthy  
mccarthy@biol.unlp.edu.ar

<sup>1</sup> Departament of Geology, University of Oviedo, C/Jesús Arias de Velasco, s/n, 33005 Oviedo, Spain

<sup>2</sup> Laboratorio de Investigaciones en Osteopatías y Metabolismo Mineral (LIOMM), Facultad de Ciencias Exactas, Universidad Nacional de La Plata, 47 y 115, 1900 La Plata, Argentina

<sup>3</sup> Centro de Estudios del Metabolismo Fosfocálcico (CeMFOC), Facultad de Medicina, Universidad Nacional de Rosario, 2000 Rosario, Argentina

utilization of this drug were implemented globally in patients with cardiovascular risk factors [6].

Bone type 1 collagen fibrils are mineralized by nanosized hydroxyapatite crystals. This tissue plays an essential role in many metabolic activities as a mineral reservoir, and several biological processes are involved in controlling bone turnover and development. These processes can be altered by an individual's health, and by genetic and environmental factors. Several analytical techniques can evaluate changes in bone mineral by analyzing its properties at different scales [7–9]. Fourier transform infrared spectroscopy is particularly useful as it provides detailed information regarding several molecular constituents of bone such as its collagen, carbonate and phosphate content [9, 10]. Morphological properties of bone in the micrometric and milimetric ranges (e.g., trabecular and cortical area, distribution and density obtained by peripheral quantitative computed tomography or pQCT, as well as bone cellularity obtained by histomorphometry or HMM) together with its chemical composition, largely determine its biomechanical properties (e.g., toughness, stiffness, and strength). In addition, crystalline characteristics (crystallite size and perfection) of apatite crystals can determine other critical properties of bone mineral (e.g., solubility, orientation degree).

The main objective of this work was to evaluate the effects of an oral treatment with SrR and/or experimental diabetes on bone composition and biomechanics, using a multi-scale approach. In addition to traditional static HMM, pQCT, and mechanical testing of long bones, we have used several analytical techniques to evaluate the chemical, crystalline, and structural properties of bone mineral, from a morphological point of view to its microstructural characterization.

## Materials and Methods

### Animal Treatments and Sample Preparation

Three-month-old male WKAH/Hok Wistar rats (190–210 g) were used. Animals were maintained in a temperature-controlled room at 23 °C, with a fixed 12-h light:12-h darkness cycle, and fed standard rat laboratory chow and water ad libitum. All experiments with animals were done in conformity with the Guidelines on Handling and Training of Laboratory Animals published by the Universities Federation for Animals Welfare [11]. Approval for animal studies was obtained from our institutional animal welfare committee (CICUAL Protocol Number 001-05-15). Partially insulin-deficient diabetes mellitus was induced in a group of ten animals by i.p. injection of nicotinamide (50 mg/kg in physiological saline), followed by i.p. streptozotocin (60 mg/kg freshly dissolved in 0.05 M citrate buffer pH 4.5) [12, 13], while another group of ten rats was allowed to remain non-diabetic.

Rats were then subdivided into four groups of five animals per group: non-treated non-diabetic (NTND) and non-treated diabetic (NTD) rats received water ad libitum, whereas strontium-treated non-diabetic (TND) and strontium-treated diabetic (TD) rats received 625 mg/kg/day of SrR (Protos, Servier, Buenos Aires, Argentina) in their drinking water for 6 weeks [14]. At the end of all experiments and prior to sacrifice, non-fasting blood samples were taken from all animals and serum was stored at –20 °C until biochemical evaluation. All rats were sacrificed under anesthesia by rapid cervical dislocation. Right femora were cleaned of soft tissue and bones were analyzed by several analytical techniques in sequential order from non-destructive to destructive procedures. First, pQCT was performed and then mechanical testing, after which, bone fragments from the diaphysis were dried to a constant weight and ground with a mill (MM200, RETSCH). The same bone powder was used for subsequent analyses: X-ray diffraction (XRD), attenuated total reflection Fourier transform infrared (FTIR) spectroscopy, and inductively coupled plasma optical emission spectrometry (ICP-OES). Left femora were fixed, decalcified, and processed for static HMM evaluation.

### HMM Examination of Long Bones

Dissected left femora were cleaned of soft tissue, fixed in 10% formalin, decalcified in 10% EDTA, and embedded in paraffin, and 5- $\mu$ m sections of the proximal secondary spongiosa were obtained with an SM 2000R Leica microtome. Sections were stained with hematoxylin-eosin (H-E) and photographed with a Nikon Coolpix 4500 digital camera on an Eclipse E400 Nikon microscope. Images were analyzed using the ImageJ program with a microscope scale plugin. In all experimental groups, relative trabecular area (TbAr) and trabecular bone osteocytic density were evaluated 250  $\mu$ m distal from the cartilage growth plate [15].

### ICP-OES Studies

Bone powder (50 mg) was dissolved in 10% HNO<sub>3</sub> (1 ml, 24 h) and 30% H<sub>2</sub>O<sub>2</sub> (1 ml, 24 h) and microwave digested. Calcium, phosphorus, magnesium, and strontium concentrations were measured using an Optima 8300 ICP-OES (Perkin Elmer). Concentrations are given in dry weight (d.w.). The precision of chemical analyses was better than 1 ppm.

### Bone Powder XRD Analyses

X-ray diffraction was performed with an X'Pert Pro (PANalytical) powder diffractometer using CuK $\alpha$  radiation produced at 40 mA and 45 kV. Scans were performed between 2 $\theta$  values of 20° and 75° with a step of 0.0042° and a count time/step of 5.08 s. Average crystallite size (*D*) of bone

crystals was calculated from (002) diffraction peak (apatite *c*-axis) using X Powder software by Scherrer equation [16]. The *D* values represent a measure of the average coherent crystal size domains and can be employed as a crystallinity index of apatite bone crystals [17].

### FTIR Spectroscopy

Infrared spectra were obtained with an FTIR JASCO. Spectra were collected from 600 to 4000  $\text{cm}^{-1}$  in absorbance mode. For each sample, 124 scans were collected at 1  $\text{cm}^{-1}$  resolution. All curve fitting was performed (and integrated areas measured) using the curve fitting software Systat Software Inc. PeakFit v4.11. The amount of phosphate, carbonate, collagen, and lipids in bone were estimated from the peak area of absorption bands associated with phosphate, carbonate, amide, and C-H aliphatic groups identified in the infrared spectra [9, 10, 18]. The degree of bone mineralization was defined as the band intensity ratios of phosphate in bone mineral to organic matrix [19] and estimated as  $A_{900-1200}/A_{1660}$ , where  $A_{900-1200}$  represents the amount of phosphate in bone and  $A_{1660}$  the amount of amide I groups (main band from bone organic matrix) [20]. This ratio is linearly correlated to the mineral content of bone (ash weight) [21]. The relative amount of carbonate in bone mineral ( $\text{MinCO}_3$ ) was calculated as the ratio of  $A_{1405}$  (carbonate type B substitution) to phosphate ( $A_{900-1200}$ ). The crystallinity index (CI) was calculated as the ratio between  $A_{1030}$  (related with highly crystalline apatite) and  $A_{1020}$  (poorly crystalline apatite) [22].

### Bone Length and pQCT Evaluation

Right femora were scanned using a Stratec XCT 960 A CT scanner with version 5.20 software (Norland Stratec Medizintechnik, Germany). The precision and accuracy of this pQCT system used has been verified previously [23]. In addition, total bone length was measured using an electronic sliding caliper with an accuracy of 0.1 mm.

Bone density values up to 500  $\text{mg cm}^{-3}$  were defined as trabecular bone (peelmode 2) and were evaluated in the metaphysis (10% point). Cortical bone was analyzed in the diaphysis, scanning at a point located 50% of the total bone length, using the parameter CORTMODE1 with a density threshold of  $>800 \text{ mg cm}^{-3}$ . The voxel size was set to 0.07 mm.

For both cortical and trabecular bone, the following parameters were determined: bone mineral content (BMC,  $\text{mg/mm}$ ), volumetric bone mineral density (vBMD,  $\text{mg/cm}^3$ ), and bone cross-sectional area (CSA,  $\text{mm}^2$ ). Additionally, for cortical bone (in the diaphysis), we also determined the following: periosteal perimeter (mm), endosteal perimeter (mm), cortical thickness (mm), and anterior-posterior cross-sectional bending second moment of inertia (xCSMI,  $\text{mm}^4$ ). xCSMI was

calculated as  $\Sigma(A_i d_i^2)$ , with  $A_i$  being the area of each individual pixel included in cortical bone tissue of the cross section (in  $\text{mm}^2$ ) and  $d_i^2$  being the squared distance of that pixel to the anterior-posterior (A-P) bending axis (*X*) of the image (in  $\text{mm}^2$ ). Thus, xCSMI grows exponentially with the distance at which cortical bone is distributed from the bending axis [23].

### Mechanical Three-Point Bending Analysis

Three-point bending test was performed on right femora (after pQCT determinations) at 50% of total bone length, using an electromechanical testing machine (Digimesh TC500) with a load cell of 500-N capacity (Interface, AZ, USA) at room temperature, with a 20-mm length span and a loading speed of 5 mm/s. Load *F* (applied in an anterior-posterior direction) and displacement *D* were recorded until rupture. The maximum force supported by the bone prior to rupture (*F*Max) was regarded as its ultimate strength. Data for each sample was used to obtain its stress-strain curve. Maximum elastic deflection (yield-point displacement *D*<sub>y</sub>) and maximum load supported elastically at yield point (*F*<sub>y</sub>) were used to calculate mid-shaft structural rigidity at yield point (*F*<sub>y</sub>/*D*<sub>y</sub>) for each sample. Toughness was defined as the amount of energy absorbed by the bone while being deformed (*E*<sub>abs</sub>) and determined as the area under the stress-strain curve. *E*<sub>abs</sub> was calculated for the elastic (pre-yield), plastic (post-yield), and total periods of bone deformation (*E*-*E*<sub>abs</sub>, *P*-*E*<sub>abs</sub>, and *T*-*E*<sub>abs</sub>).

### Statistical Analysis

Averages of the data per rat and group were calculated, and bone variables are expressed as the mean  $\pm$  SEM. One-way ANOVA and simple regression were employed to evaluate the differences between grouped data and the associations between variables. Differences were considered significant at  $p < 0.05$ . Statistical analysis was performed using SPSS (SPSS Inc., Chicago, IL, USA) and/or Statistica software (StatSoft, USA).

## Results

### Glucose Metabolism, Body Weight, and Femoral Length

Non-fasting plasma glucose was  $1.46 \pm 0.15 \text{ g/l}$  for non-diabetic rats, versus  $3.67 \pm 0.44 \text{ g/l}$  for diabetic animals. Insulin levels were  $1.31 \pm 0.15 \text{ ng/ml}$  in non-diabetic rats and  $0.27 \pm 0.15 \text{ ng/ml}$  in diabetic animals. Oral treatment with SrR did not further modify plasma glucose or insulin levels. As can be seen in Table 1, the mean weight of diabetic rats was 12 to 15% lower than that of non-diabetic animals, although

**Table 1** Effects of diabetes (D) and/or strontium ranelate treatment (T) on body weight and femoral length measurements. Values are expressed as the mean  $\pm$  SEM

	NTND	TND	NTD	TD
Body weight (g)	324 $\pm$ 43	332 $\pm$ 54	284 $\pm$ 55	288 $\pm$ 64
Femoral length (mm)	36.0 $\pm$ 1.0	35.8 $\pm$ 1.1	35.8 $\pm$ 0.8	35.2 $\pm$ 1.5

this difference was not significant. No differences between groups were observed for femoral length measurements.

### Bone Crystallite Properties and Mineral Composition

As can be seen in Fig. 1, XRD measurement of apatite crystallite sizes did not show significant differences between groups. Bone mineral composition was further evaluated by FTIR and ICP-OES.

By ICP-OES analysis (Table 2), we found no differences between all experimental groups for calcium and phosphorous elemental analyses, nor in the Ca/P ratio (a sensitive measure of bone mineral changes). However, there was a non-significant tendency for Ca/P ratio to decrease in diabetic groups (NTD and TD) versus non-diabetic animals (NTND and TND). As expected, SrR treatment significantly increased the levels of strontium incorporated into bone mineral. Interestingly, bones from diabetic animals tended non-significantly to incorporate higher levels of strontium (TD versus TND).

Table 2 (FTIR analysis) shows the results for absorption bands associated with phosphate (A900–1200) and carbonate (A1405) chemical environments, type 1 collagen (A1660), as well as several bone parameters that describe mineral composition. The crystallinity index (ratio between highly and poorly crystalline phosphate) was significantly lower for the TD group (versus TND). The ratio between carbonate and

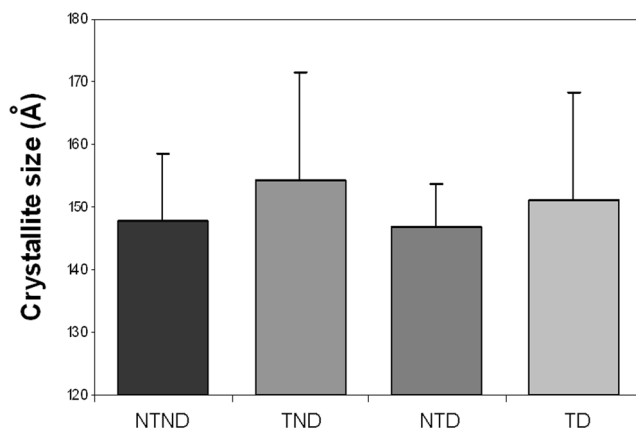


**Fig. 1** Effects of diabetes and/or strontium ranelate treatment on crystallite size determined by X-ray diffraction (XRD) analyses. Values are expressed as the mean  $\pm$  SEM

phosphate content ( $\text{MinCO}_3^-$ ) was significantly decreased in groups NTD and TD (versus group TND).

### pQCT Measurements

In the femoral metaphysis (Table 3), induction of diabetes tended non-significantly to decrease all parameters of trabecular bone evaluated by pQCT (NTD versus NTND). Treatment of diabetic animals with SrR (group TD) worsened these effects of Diabetes, with a significant decrease versus NTND for trabecular BMC, vBMD and CSA. However, treatment of non-diabetic animals with SrR had no such effect.

At the femur mid-shaft (Table 3), induction of diabetes was associated with a significant decrease in cortical BMC, cortical thickness, and periosteal perimeter (NTD and TD, versus NTND and TND). SrR treatment did not induce any additional effects on these parameters for cortical bone. No significant inter-group differences were observed for xCSMI data. In order to relate the mass of cortical tissue with its distribution (geometry), mid-shaft xCSMI was plotted against cortical BMC for each sample and experimental group (Fig. 2). Positive regression lines were obtained for every group. All lines were virtually parallel, although their intercepts differed significantly (ANCOVA, global  $p < 0.001$ ). Results for TND and TD groups fell on different portions of the same line: TD showed lower values of BMC than TND, although both groups had the same xCSMI/BMC ratio. Regression lines showed a progressive displacement: NTND group to the right, TND and TD groups in the middle, and NTD animals to the left.

### HMM Analysis

Changes observed in HMM-assessed TbAr of the metaphyseal secondary spongiosa were similar to those obtained by pQCT for metaphyseal trabecular cross-sectional area. Thus, TbAr values tended non-significantly to diminish in NTD animals and were significantly decreased in TD rats versus NTND (Fig. 3a). Interestingly, NTD rats (versus NTND) showed a significant decrease in trabecular bone osteocyte density (Fig. 3b), an effect that was completely prevented by SrR treatment (TD group).

### Mechanical Testing

NTD rats showed a significant decrease in the maximal load supported elastically at yield ( $F_y$ ) when compared with NTND animals. SrR treatment further impaired this parameter in diabetic rats, but not in non-diabetic animals (Fig. 4a). Diaphyseal structural rigidity during the elastic phase ( $F_y/D_y$ ) was significantly increased in TD animals versus all other groups (Fig. 4b). Ultimate bone strength ( $F_{\text{Max}}$ ) was significantly decreased in NTD group versus both NTND and TND groups (Fig. 4c). This impairment was partially prevented by



**Table 2** Effects of diabetes (D) and/or strontium ranelate treatment (T) on femoral diaphysis bone mineral composition parameters measured by inductively coupled plasma optical emission spectrometry (ICP-OES) and attenuated total reflection Fourier transform infrared (ATR-FTIR) spectroscopy. *MinCO<sub>3</sub>* relative amount of carbonate in bone mineral. Values are expressed as the mean  $\pm$  SEM

	NTND	TND	NTD	TD
ICP-OES analysis				
Ca/P	1.93 $\pm$ 0.15	1.93 $\pm$ 0.08	1.85 $\pm$ 0.09	1.86 $\pm$ 0.05
Sr (ppm)	0.36 $\pm$ 0.04	5.85 $\pm$ 1.80****	0.34 $\pm$ 0.02	7.64 $\pm$ 2.13****
FTIR analysis				
A900–1200	27.49 $\pm$ 1.11	27.49 $\pm$ 1.56	25.53 $\pm$ 3.51	27.67 $\pm$ 3.80
A1405	3.71 $\pm$ 0.25	3.76 $\pm$ 0.25	3.19 $\pm$ 0.43	3.41 $\pm$ 0.44
A1660	4.41 $\pm$ 0.26	4.82 $\pm$ 0.38	4.01 $\pm$ 0.67	4.27 $\pm$ 0.56
Degree of mineralization	6.239 $\pm$ 0.209	5.720 $\pm$ 0.400	6.404 $\pm$ 0.341	6.485 $\pm$ 0.329
MinCO <sub>3</sub>	0.135 $\pm$ 0.006	0.137 $\pm$ 0.004	0.125 $\pm$ 0.003**	0.124 $\pm$ 0.009**
Crystallinity Index	0.560 $\pm$ 0.027	0.578 $\pm$ 0.020	0.556 $\pm$ 0.027	0.528 $\pm$ 0.010**

\* $p < 0.01$  versus NTND; \*\* $p < 0.05$  versus TND; \*\*\* $p < 0.05$  versus NTD

SrR treatment (TD group). Diaphyseal total structural toughness (T-Eabs) decreased significantly in all diabetic and SrR-treated groups (Fig. 4d). Homologous decreases in toughness were observed for the plastic phase of deformation (P-Eabs), but not its elastic phase (E-Eabs).

## Discussion

Diabetes mellitus is a chronic metabolic disease that in the long-term may affect bone tissue, a complication called diabetic osteopenia. These diabetes-induced alterations of bone include alterations in bone mineral content and density (osteopenia and/or osteoporosis) and increased fracture risk coupled with a decrease in fracture repair [24, 25]. Although some investigators have reported a positive clinical outcome after treating diabetic patients with anti-osteoporotic drugs [26], other authors have warned about a possible resistance in diabetic individuals to long-term treatment with agents such as bisphosphonates [27]. More than a decade ago, use of SrR was

approved for treatment of postmenopausal osteoporosis in several countries (not the USA); however, there has been scant research regarding the effects of this drug on bone metabolism in the context of diabetes mellitus. In view of restrictions imposed on the use of SrR after a negative report by the European Pharmacovigilance Risk Assessment Committee [6], this drug was discontinued by Servier as of August 2017. However, SrR was used for more than 10 years as part of first-line anti-osteoporotic therapy in many countries. In this sense, knowledge of the effects of strontium accumulation in bone tissue could be of great relevance to predict future possible side effects of this drug in patients previously treated with strontium, with or without additional pathologies such as diabetes.

## Effects of Diabetes and/or SrR on Biometric Parameters and Bone Extracellular Composition

In uncompensated insulin-deficient diabetes, there is a global negative energy balance partly due to persistent glycosuria, which is associated with weight loss. In our present study,

**Table 3** Peripheral quantitative computed tomography (pQCT) femoral measurements for cortical bone at diaphysis (50%, mid-shaft), and for trabecular bone at proximal metaphysis (10% of bone length). Values are expressed as the mean  $\pm$  SEM

	NTND	TND	NTD	TD
Cortical—50%				
Cortical BMC	11.47 $\pm$ 0.67	11.62 $\pm$ 0.78	9.65 $\pm$ 1.62***	9.66 $\pm$ 1.34***
Cortical vBMD	1326.5 $\pm$ 15.7	1338.4 $\pm$ 2.9	1302.60 $\pm$ 23.61	1310.58 $\pm$ 43.19
Cortical CSA	8.65 $\pm$ 0.43	8.68 $\pm$ 0.57	7.39 $\pm$ 1.12	7.35 $\pm$ 0.85
Cortical thickness	0.87 $\pm$ 0.04	0.89 $\pm$ 0.06	0.75 $\pm$ 0.09***	0.77 $\pm$ 0.04***
Periosteal perimeter	12.66 $\pm$ 0.21	12.56 $\pm$ 0.19	12.40 $\pm$ 0.23***	12.42 $\pm$ 0.04***
Endocortical perimeter	7.18 $\pm$ 0.21	6.97 $\pm$ 0.23	7.43 $\pm$ 0.64	7.66 $\pm$ 0.90
xCSMI	7.33 $\pm$ 0.79	8.31 $\pm$ 1.18	7.30 $\pm$ 1.20	7.10 $\pm$ 0.61
Trabecular—10%				
Trabecular BMC	0.97 $\pm$ 0.18	1.20 $\pm$ 0.58	0.62 $\pm$ 0.20	0.37 $\pm$ 0.16****
Trabecular vBMD	207.1 $\pm$ 32.6	235.9 $\pm$ 76.5	143.14 $\pm$ 37.8	109.8 $\pm$ 28.4****
Trabecular CSA	4.68 $\pm$ 0.40	5.04 $\pm$ 0.97	4.26 $\pm$ 0.49	3.27 $\pm$ 0.61****

\* $p < 0.05$  versus NTND; \*\* $p < 0.05$  versus TND; \*\*\* $p < 0.01$  versus TND

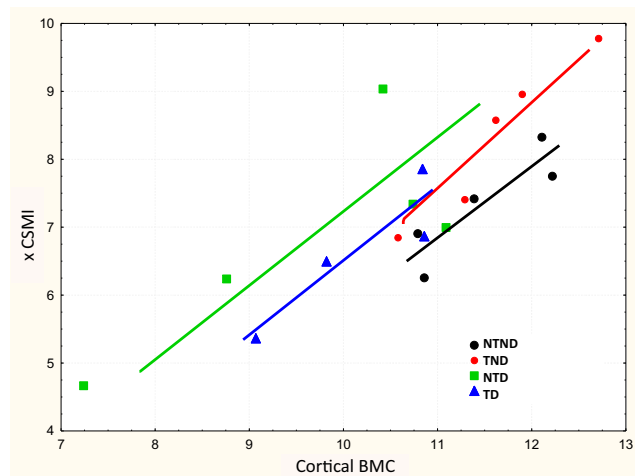


**Fig. 2** Linear regression curves obtained for anterior-posterior cross-sectional bending second moment of inertia (xCSMI) versus cortical bone mineral content (BMC), for each experimental group

diabetic animals after 6 weeks showed a lower (though non-significantly different) weight gain when compared to non-diabetic groups. This biometric parameter has been proposed to be a predictor of changes in the macro-structure of bones; however, we found no differences in femoral length measurements between groups. On a chemical scale, the Ca/P ratio of

bone mineral is considered to be a sensitive measure of bone mineral quality. Previous results by other authors have shown that there is a relationship between bone loss and a diminished Ca/P ratio [28]. In our present study, by ICP-OES analysis, we found a tendency to decrease in the Ca/P ratio of diabetic versus non-diabetic groups, which though non-significant, could be suggestive of underlying defects in bone mineralization. The apatite lattice possesses considerable tolerance for a wide range of substituents, thus allowing the incorporation of  $\text{Sr}^{2+}$  into the bone mineral structure. According to previous studies, most of the  $\text{Sr}^{2+}$  loaded on bone mineral is believed to be exchanged or adsorbed onto the crystal surface [29]. Our present results demonstrate that in SrR-treated animals (groups TND and TD),  $\text{Sr}^{2+}$  was predictably incorporated into bone mineral; and this incorporation was found to be greater in diabetic rats than in non-diabetic animals. In spite of this strontium incorporation, our results obtained by XRD analysis show that apatite crystallite sizes did not differ between experimental groups after a 6-week SrR treatment.

An interesting approach to study bone quality is FTIR spectrometry, which has been previously used to analyze alterations in bone mineral composition due to pathological conditions such as diabetes mellitus [30, 31]. In our present study, FTIR spectral analysis indicated that inorganic environments associated with phosphate mineral ( $\nu_1$ ,  $\nu_3$   $\text{PO}_4^{3-}$  area contours) were altered by diabetes and/or SrR treatment. Specifically, the crystallinity index (ratio of  $1030\text{ cm}^{-1}$ /  $1020\text{ cm}^{-1}$  bands, which respectively represent phosphate components in a stoichiometric and non-stoichiometric apatite environment and are directly related to crystal maturity) showed the lowest values for TD rats. In addition, the ratio of carbonate mineral to phosphate content ( $\text{MinCO}_3$ ) was significantly decreased in NTD animals, and even more so in the TD group. Interestingly, other investigators have previously found that both the Crystallinity Index and the carbonate/phosphate ratio increase over time in healthy bones [32], whereas in diabetic rats, there is a decrease in the carbonate/phosphate ratio of long bones [33]. In addition, a reduction in the carbonate content of bone mineral has also been previously associated with osteoporosis [34].

### Effects of Diabetes and/or SrR Treatment on Bone Mass and Cellularity

Other authors have observed a decrease in trabecular bone associated with diabetes [35, 36]. In addition, previous studies have also found a decrease of cortical bone thickness in diabetic rats [29], and a reduction in the periosteal perimeter at the tibia and radius mid-shaft associated with increased serum levels of adipokines in patients with type 2 diabetes [37]. Our present results support these previous reports. We have found that (a) trabecular area, BMC, and vBMD tended to decrease in NTD animals, and were significantly diminished in TD rats,

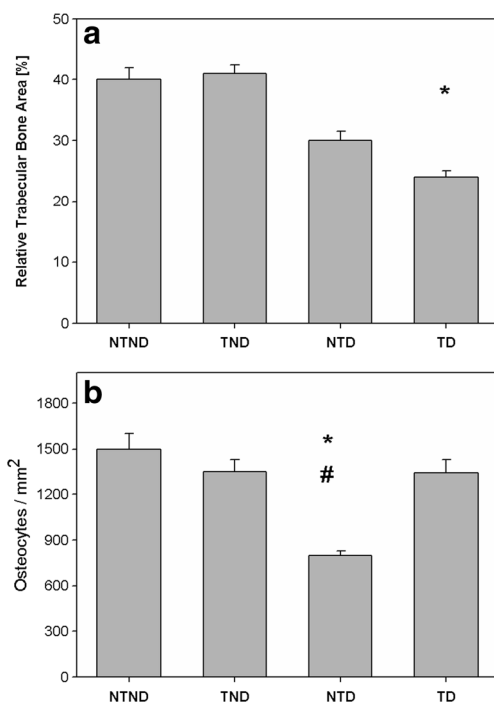
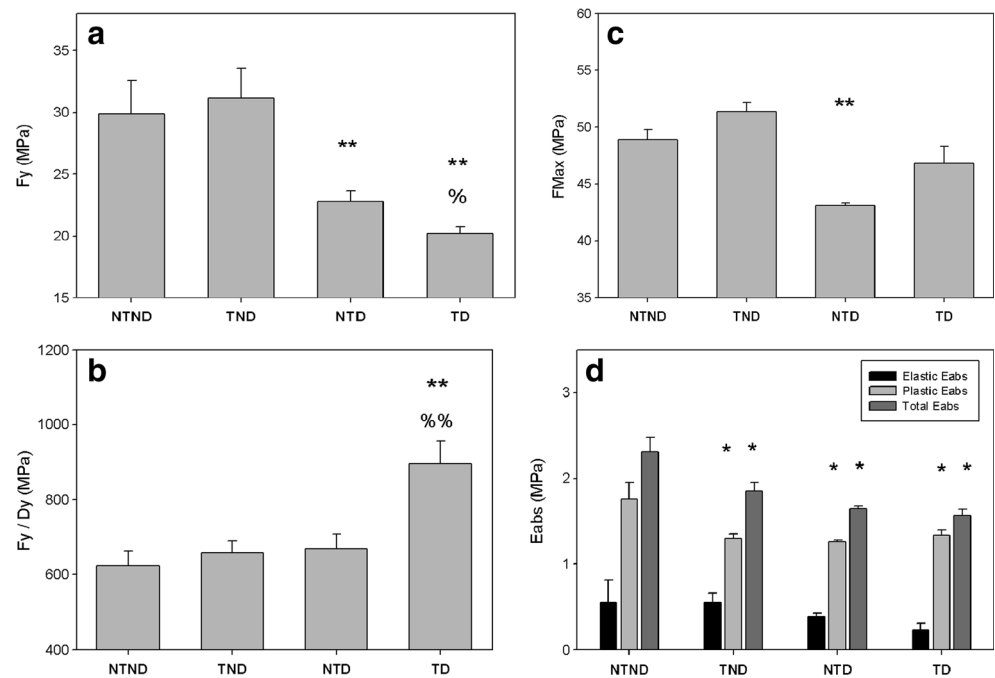


**Fig. 3** Histomorphometric analysis of the proximal secondary spongiosa for left femora of all animals from each experimental group. **a** Relative trabecular bone area, expressed as a percentage of total area. **b** Osteocyte density of trabecular bone, expressed as cell number per square millimeter of trabecular bone. Values are expressed as the mean  $\pm$  SEM. \* $p < 0.01$  versus NTND and versus TND; # $p < 0.01$  versus TD

**Fig. 4** Results obtained from femoral mechanical testing (three-point bending analyses) of all animals from each experimental group. **a** Maximum load supported elastically at yield point (Fy). **b** Structural rigidity of the diaphysis during the elastic phase (Fy/Dy). **c** Maximal force supported by the bone prior to rupture (FMax). **d** Bone toughness was calculated as the area under the stress-strain curve, and determined for the elastic (pre-yield), plastic (post-yield until rupture), and total periods of bone deformation (E-Eabs, P-Eabs, T-Eabs). Values are expressed as the mean  $\pm$  SEM. \* $p < 0.05$  versus NTND; \*\* $p < 0.01$  versus NTND; % $p < 0.05$  versus NTD; %% $p < 0.01$  versus NTD



and (b) cortical BMC and thickness were significantly decreased for both NTD and TD groups, in which a mild but significant delay of bone growth-in-width (as assessed by periosteal perimeter values) could also be observed.

A structural alteration of the osteocyte network can impair bone biomechanical response to strains and/or the ability of bone to repair peri-lacunar micro-damage [38]. Previous studies have shown that experimental Diabetes can reduce the osteocyte density of trabecular bone [36]. Our present results support those findings and additionally indicate that SrR treatment can prevent this deleterious effect of diabetes. Although we have not evaluated any mechanisms of cell death in this study, the observed decrease in osteocyte density of non-treated diabetic animals could have been due to increased apoptosis, an effect that might have been prevented by SrR treatment. We have previously shown that  $\text{Sr}^{2+}$  can prevent anti-proliferative actions induced by advanced glycation end-products (AGEs) on cultured osteoblasts [39]. AGEs accumulate in the extracellular matrix of diabetic tissues (including bone) due to both hyperglycemia and oxidative stress, have been implicated in the pathogenesis of diabetic osteopenia and could be the mediators of osteocyte loss in bones from diabetic animals observed in the present and previous studies [36]. The diabetes-induced decrease in osteocyte density could also be due to a diminished capacity of bone marrow stromal cells to undergo osteoblastic progression (and thus eventually become functional osteocytes). Interestingly, we have recently found that while experimental diabetes decreases the osteogenic potential of bone marrow stromal cells, a 6-week treatment of diabetic animals with SrR can completely prevent this effect [40].

### Effects of Diabetes and/or SrR Treatment on Bone Geometry and Mechanical Properties

The structural properties of a femur shaft in A-P bending (whole-bone stiffness, toughness, strength) depend both on cortical mechanical quality (intrinsic stiffness and toughness), and on cortical mass and spatial distribution (BMC, area, periosteal and endocortical perimeters, thickness, xCSMI). In our present study, no significant changes were observed for cCSMI (considered a specific indicator of diaphyseal cross-sectional geometry for bending and proposed to be under osteocyte control through the bone mechanostat mechanism) [41]. However, when we evaluated a possible association between cortical mineral mass (BMC) and its distribution (xCSMI), we observed positive linear correlations between these variables for each experimental group. In spite of a considerable dispersion of xCSMI values, the cortical xCSMI/BMC ratio (slope) for each group was always constant, and almost coincident between groups. Therefore, the mechanical impact of changes in cortical bone shell properties may be attributed to effects on bone mass rather than distribution.

By mechanical analysis, we found that diabetes per se induced a significant decrease in femoral diaphysis ultimate strength at rupture (FMax). This effect may be partially due to an impairment in cortical bone mineralized mass, perhaps related to delayed growth-in-width. Interestingly, during the plastic (post-yield) period, bones from diabetic animals were significantly more brittle (i.e., showed lower P-Eabs values) than their non-diabetic counterparts, an effect that is consistent with their reduction in cortical mass and could also explain the diabetes-induced decrease in FMax. Nevertheless, this by no

means rules out possible negative effects on other microstructural determinants of bone mechanical “quality.”

Diabetes has been described to increase bone stiffness and, perhaps as a result of that, can impair bone toughness through effects on collagen lattice and crystal size, shape, and arrangement [24]. A previous study with spontaneously diabetic rats reported impaired torsional strength, angular deformation, and energy absorption, with little or no change in BMC and BMD [35]. Interestingly, our results show that while femora from diabetic animals had a significant increase in poorly crystalline apatite and a lower carbonate/phosphate ratio, there were no changes in their vBMD (an acknowledged indicator of bone stiffness) [23]. In addition, the yielding strength ( $F_y$ ) of bones was significantly lower in diabetic than in non-diabetic rats, while structural diaphyseal stiffness ( $F_y/D_y$ ) of non-treated diabetic animals was unaffected throughout the elastic phase. These two findings are difficult to explain in view of the absence of effects on both cortical vBMD and pre-yield toughness (E-Eabs). However, diabetes can enhance bone tissue stiffness through mechanisms which may be unrelated to mineralization (e.g., an increase in type 1 collagen AGEs-crosslinking).

Previous *in vivo* studies with non-diabetic animals have demonstrated that SrR administration can improve bone mass, microarchitecture, and fracture resistance, and also prevent bone loss [42, 43]. In our study, TND animals showed a significant decrease (versus NTND group) in bone plastic and total structural toughness (P-Eabs and T-Eabs) without any effect on bone pre-yield properties ( $F_y/D_y$  or  $F_y$ ) and additionally no significant effects on bone ultimate strength ( $F_{max}$ ). The effects of SrR treatment on bone structural toughness are difficult to explain, especially taking into account the fact that we were unable to find alterations in bone mass, geometry, or mineralization for this experimental group.

In diabetic rats, SrR treatment (TD group) exerted some apparently paradoxical effects. To begin with, versus NTD animals it further impaired the maximum load supported elastically at yield ( $F_y$ ) without any significant effects on bone tissue mass (cortical BMC), mineralization (cortical vBMD), or distribution (periosteal and endocortical perimeters, cortical thickness, xCSMI). Additionally, TD animals (versus NTD) showed an increase in diaphyseal stiffness at yield ( $F_y/D_y$ ) without changes in bone toughness at any structural level (E-Eabs, P-Eabs, T-Eabs) and a partial prevention of the diabetes-induced impairment of bone ultimate strength ( $F_{max}$ ). The combined result of all these effects would indicate that femoral mid-shafts of TD rats were less elastic, while showing greater resistance to rupture, than those of NTD group.

## Conclusions

In the present study, we have evaluated whether experimental insulin-deficient diabetes and/or an oral treatment with SrR

can affect the mineral composition and biomechanics of femoral bone. We used several analytical techniques to characterize bone properties at different scales. We found a considerable disruption of bone induced by diabetes: a decrease in femoral apatite inorganic composition ( $\text{CO}_3^{2-}/\text{PO}_4^{3-}$  ratio), in cortical thickness and BMC, in trabecular osteocyte density, in maximum load supported at fracture and at yield point, and in overall toughness at mid-shaft. Treatment of diabetic animals with SrR worsened several parameters of bone (some of which were already impaired by diabetes):  $\text{PO}_4^{3-}$  chemical environment of apatite crystallinity; trabecular area, BMC, and vBMD; maximum load at yield point; and structural elastic rigidity. However, SrR was also able to prevent the diabetes-induced decreases in trabecular osteocyte density (completely) and in bone ultimate strength at rupture (partially). Our results have the intrinsic limitations of any rodent experimental model. However, if some of the effects reported here could be extrapolated to a clinical setting, they would indicate that strontium incorporated into bone can prevent some structural mechanical properties as previously affected by Diabetes, but not others (which may even be worsened).

**Acknowledgements** P.A-LL is an Ad Interim Assistant Professor of Crystallography and Mineralogy (UNIOVI), University of Oviedo, Spain. JMF, JLF, RC, and MSM are Members of Carrera del Investigador Científico (CONICET), Argentina. AMC is a Member of Carrera del Investigador Científico (CICPBA), Argentina. ABL is a Fellow of ANPCyT, Argentina. ADM is full Professor of Clinical Chemistry at National University of La Plata (UNLP). Financial support for this study was provided by Santander Foundation JPI-2014, CGL2015-64683-P, UNOV-13-EMERG-08, Agencia Nacional de Promoción Científica y Tecnológica (PICT 2012-0053), and grants from CONICET, CICPBA, and UNLP. We thank Dr. L.P. Olivar-Pérez (Osakidetza) for her valuable comments in preparing the manuscript.

## Compliance with Ethical Standards

**Conflict of Interest** The authors declare that they have no conflicts of interest.

## References

1. Janghorbani M, Van Dam RM, Willett WC, Hu FB (2007) Systematic review of type 1 and type 2 diabetes mellitus and risk of fracture. *Am J Epidemiol* 166:495–505
2. Bonnelye E, Chabadel A, Saltel F, Jurdic P (2008) Dual effect of strontium ranelate: stimulation of osteoblast differentiation and inhibition of osteoclast formation and resorption *in vitro*. *Bone* 42:129–138
3. Dahl SG, Allain P, Marie PJ, Mauras Y, Boivin G, Ammann P, Tsouderos Y, Delmas PD, Christiansen C (2001) Incorporation and distribution of strontium in bone. *Bone* 28:446–453
4. Meunier PJ, Roux C, Seeman E, Ortolani S, Badurski JE, Spector TD, Cannata J, Balogh A, Lemmel EM, Pors-Nielsen S, Rizzoli R, Genant HK, Reginster JY (2004) The effects of strontium ranelate on the risks of vertebral fracture in women with postmenopausal osteoporosis. *N Engl J Med* 350:459–468



5. Reginster JY, Seeman E, De Vernejoul MC, Adami S, Compston J, Phenekos C, Devogelaer JP, Curiel MD, Sawicki A, Goemaere S, Sorensen OH, Felsenberg D, Meunier PJ (2005) Strontium ranelate reduces the risk of nonvertebral fractures in postmenopausal women with osteoporosis: Treatment of Peripheral Osteoporosis (TROPOS) Study. *J Clin Endocrinol Metab* 90:2816–2822
6. Reginster JY, Brandi ML, Cannata-Andía J, Cooper C, Cortet B, Feron JM, Genant H, Palacios S, Ringe JD, Rizzoli R (2015) The position of strontium ranelate in today's management of osteoporosis. *Osteoporos Int* 26:1667–1671
7. Peters F, Schwarz K, Eppler M (2000) The structure of bone studied with synchrotron X-ray diffraction, X-ray absorption spectroscopy and thermal analysis. *Thermochim Acta* 361:131–138
8. Hassenkam T, Fantner GE, Cutroni JA, Weaver JC, Morse DE, Hansma PK (2004) High-resolution AFM imaging of intact and fractured trabecular bone. *Bone* 35:4–10
9. Boskey AL, Mendelsohn R (2005) Infrared spectroscopic characterization of mineralized tissues. *Vib Spectrosc* 38:107–114
10. Gadaleta SJ, Paschalis EP, Betts F, Mendelsohn R, Boskey AL (1996) Fourier transform infrared spectroscopy of the solution mediated conversion of amorphous calcium phosphate to hydroxyapatite: new correlations between X-ray diffraction and infrared data. *Calcif Tissue Int* 58:9–16
11. Guidelines on Handling and Training of Laboratory Animals (2011) In: Purl UFA (ed) The Biological Council of Animal Research, Welfare Panel. Guide for the care and use of laboratory animals: Eighth Edition. The National Academies Press, Washington D.C.
12. Tahara A, Matsuyama-Yokono A, Nakano R, Someya Y, Shibasaki M (2008) Hypoglycaemic effects of antidiabetic drugs in streptozotocin-nicotinamide-induced mildly diabetic and streptozotocin-induced severely diabetic rats. *Basic Clin Pharmacol Toxicol* 103:560–568
13. Skudelski T (2012) Streptozotocin-nicotinamide-induced diabetes in the rat. Characteristics of the experimental model. *Exp Biol Med* (Maywood) 237:481–490
14. Bain SD, Jerome C, Shen V, Dupin-Roger I, Ammann P (2009) Strontium ranelate improves bone strength in ovariectomized rat by positively influencing bone resistance determinants. *Osteoporos Int* 20:1417–1428
15. Sedlinsky C, Molinuevo MS, Cortizo AM, Tolosa MJ, Felice JJ, Sbaraglini ML, Schurman L, McCarthy AD (2011) Metformin prevents anti-osteogenic in vivo and ex vivo effects of rosiglitazone in rats. *Eur J Pharmacol* 668:477–485
16. Scherrer WN, Jenkins T (1983) Profile fitting for quantitative. Analysis in X-ray powder diffraction. *Adv X-ray Anal* 26:141
17. Boskey AL, Moore DJ, Amling M, Canalis E, Delany AM (2003) Infrared analysis of the mineral and matrix in bones of osteonectin-null mice and their wildtype controls. *J Bone Miner Res* 18:1005–1111
18. Paschalis EP, Jacenk O, Olsen B, Mendelsohn R, Boskey AL (1996) Fourier transform infrared microspectroscopic analysis identifies alterations in mineral properties in bones from mice transgenic for type X collagen. *Bone* 19:151–156
19. Pienkowski D, Doers TM, Monier-Faugere MC, Geng Z, Camacho NP, Boskey AL, Malluche HH (1997) Calcitonin alters bone quality in beagle dogs. *J Bone Miner Res* 12:1936–1943
20. Boskey AL (1999) Mineralization, structure and function of bone. In: Seibel MJ, Robins SP, Bilezikian JP (eds) Dynamics of bone and cartilage metabolism. Academic Press, San Diego, pp 153–164
21. Faibish D, Gomes A, Boivin G, Binderman I, Boskey A (2005) Infrared imaging of calcified tissue in bone biopsies from adults with osteomalacia. *Bone* 36:6–12
22. Miller LS, Vairavamurthy V, Chance MR, Mendelsohn R, Paschalis EP, Betts F, Boskey AL (2001) In situ analysis of mineral content and crystallinity in bone using infrared micro-spectroscopy of the  $\nu_4$  PO<sub>4</sub>- vibration. *Biochim Biophys Acta* 1527:11–19
23. Capozza RF, Mondelo N, Reina PS, Nocciolino L, Meta M, Roldan EJA, Ferretti JL, Cointry GR (2013) Mineralization- and remodeling-unrelated improvement of the post-yield properties of rat cortical bone by high doses of olpadronate. *J Musculoskeletal Neuronal Interact* 13:185–194
24. Nyman JS (2013) Effects of diabetes on the fracture resistance of bone. *Clinic Rev Bone Miner Metab* 11:38–48
25. Schwartz AV (2016) Epidemiology of fractures in type-2 diabetes. *Bone* 82:2–8
26. Keegan TH, Schwartz AV, Bauer DC, Sellmeyer DE, Kelsey JL (2004) Effect of alendronate on bone mineral density and biochemical markers of bone turnover in type 2 diabetic women: the fracture intervention trial. *Diabetes Care* 27:1547–1553
27. Dagdelen S, Sener D, Bayraktar M (2007) Influence of type 2 diabetes mellitus on bone mineral density response to bisphosphonates in late postmenopausal osteoporosis. *Adv Ther* 24:1314–1320
28. Tzaphlidou M (2008) Bone architecture: collagen structure and calcium/phosphorus maps. *J Biol Phys* 34:39–49
29. Farlay D, Panczer G, Rey C, Delmas PD, Boivin G (2010) Mineral maturity and crystallinity index are distinct characteristics of bone mineral. *J Bone Miner Metab* 28:433–445
30. Alvarez-Lloret P, Lind PM, Nyberg I, Örborg J, Rodríguez-Navarro AB (2009) Effects of 3,3',4,4',5-pentachlorobiphenyl (PCB126) on vertebral bone mineralization and on thyroxine and vitamin D levels in Sprague-Dawley rats. *Toxicol Lett* 187:63–68
31. Donmez BO, Unal M, Ozdemir S, Ozturk N, Oguz N, Akkus O (2016) Effects of losartan treatment on the physicochemical properties of diabetic rat bone. *J Bone Miner Metab* 35:161–170. <https://doi.org/10.1007/s00774-016-0748-9>
32. Boskey A, Camacho NP (2007) FT-IR imaging of native and tissue-engineered bone and cartilage. *Biomaterials* 28:2465–2478
33. Boyar H, Turan B, Severcan F (2003) FTIR spectroscopic investigation of mineral structure of streptozotocin induced diabetic rat femur and tibia. *Spectroscopy* 17:627–633
34. Thompson DD, Posner AS, Laughlin WS, Blumenthal NC (1983) Comparison of bone apatite in osteoporotic and normal Eskimos. *Calcif Tissue Int* 35:392–393
35. Verhaeghe J, Suiker AMH, Einhorn TA, Geusens P, Visser WJ, van Herck E, van Bree R, Magitsky S, Bouillon R (1994) Brittle bones in spontaneously diabetic female rats cannot be predicted by bone mineral measurements: studies in diabetic and ovariectomized rats. *J Bone Miner Res* 9:1657–1667
36. Tolosa MJ, Chuguransky SR, Sedlinsky C, Schurman L, McCarthy AD, Molinuevo MS, Cortizo AM (2013) Insulin-deficient diabetes-induced bone microarchitecture alterations are associated with a decrease in the osteogenic potential of bone marrow progenitor cells: preventive effects of metformin. *Diabetes Res Clin Pract* 101:177–186
37. Petit MA, Paudel ML, Taylor BC, Hughes JM, Strotmeyer ES, Schwartz AV, Cauley JA, Zmuda JM, Hoffman AR, Ensrud KE (2010) Bone mass and strength in older men with type 2 diabetes: the Osteoporotic Fractures in Men Study. *J Bone Miner Res* 25:285–291
38. Ferretti JL, Cointry GR, Capozza RF (2014) Osteocitos mirando hacia arriba. *Actual Osteol* 10:43–80
39. Fernández JM, Molinuevo MS, Sedlinsky C, Schurman L, Cortizo AM, McCarthy AD (2013) Strontium ranelate prevents the deleterious action of advanced glycation endproducts on osteoblastic cells via calcium channel activation. *Eur J Pharmacol* 706:41–47

40. Lino AB, Fernández JM, Molinuevo MS, Cortizo AM, McCarthy AD (2016) In vivo effects of strontium ranelate on bone marrow progenitor cells of diabetic rats. *Actual Osteol* 12: 78–86
41. Lerebours C, Buenzli PR (2016) Towards a cell-based mechanostat theory of bone: the need to account for osteocyte desensitisation and osteocyte replacement. *J Biomech* 49: 2600–2606
42. Mieczkowska A, Mansur SA, Irwin N, Flatt PR, Chappard D, Mabilieu G (2015) Alteration of the bone tissue material properties in type 1 diabetes mellitus: a Fourier transform infrared microspectroscopy study. *Bone* 76:31–39
43. Boyd SK, Szabo E, Ammann P (2011) Increased bone strength is associated with improved bone microarchitecture in intact female rats treated with strontium ranelate: a finite element analysis study. *Bone* 48:1109–1116